Effect of the Bulky Side Chain on the Backbone Structure of the Amino Acid Derivative Valinamide

Richard J. Lavrich,† Charles R. Torok, and Michael J. Tubergen*

Department of Chemistry, Kent State University, Kent, Ohio 44242-0001

Received: March 7, 2002; In Final Form: May 24, 2002

Rotational spectra have been recorded for five isotopic species of valinamide, the amide derivative of the amino acid valine. The rotational constants for the normal species are $A = 3019.242(1)$ MHz, $B = 1473.0587(7)$ MHz, and $C = 1252.5350(8)$ MHz. Ab initio calculations at the MP2/6-31G** level identified six conformational minima with three different orientations of the isopropyl side chain and two different intramolecular hydrogen bonding interactions. None of the theoretical structures reproduces the fifteen experimental moments of inertia derived from the rotational constants. Least-squares fits of the theoretical structure with $\chi_1 = 300°$ and an amide-to-amine intramolecular hydrogen bond find that the amino amide backbone torsional angle Ψ increases from $-9.3°$ to $+9.7(30)°$. The nitrogen atomic coordinates of the least-squares-fit structure were found to be in agreement with the coordinates calculated using Kraitchman's equations for single isotopic substitution, but the nitrogen coordinates of the theoretical structures were significantly different from the Kraitchman coordinates.

Introduction

Weak intermolecular hydrogen bonds are believed to be the basis of the activities of molecules involved in biochemical processes. The low binding energies of these hydrogen bonds, typically 10−30 kJ mol^{-1}, allow the biomolecules to interact with their targets before breaking free. Nearly all biochemically relevant molecules contain intramolecular hydrogen bonding interactions as well. Biochemical processes therefore involve a combination of intra- and intermolecular hydrogen bonding interactions, the details of which are not always well understood. Gas-phase spectroscopy provides an excellent opportunity to isolate these interactions: the study of monomers of biomolecules allows for the examination of the intramolecular hydrogen bonding interaction free from the perturbations of intermolecular hydrogen bonds, and the formation of their van der Waals complexes introduces intermolecular interactions.

Amino acids are among the simplest biomolecules that contain intramolecular hydrogen bonds, and they serve as building blocks of more complex peptides and proteins. Accurate structure determination and the identification of intramolecular hydrogen bonding motifs in these systems may provide insight into the interactions in larger systems as well as to provide valuable experimental data for testing and refining ab initio methods. Spectroscopic studies of amino acids have been hampered, however, by difficulties in obtaining suitable number densities in the gas phase. As a result, structures for only two amino acids, glycine and alanine, have been determined. Microwave spectroscopy,[1−6] electron diffraction,[7,8] and matrix isolation spectroscopy[9−11] have identified up to three stable conformations of glycine and alanine, each stabilized by a different intramolecular hydrogen bonding network. The lowest energy conformation of glycine and alanine is stabilized by a bifurcated intramolecular hydrogen bond from the amino hydrogens to the carboxyl oxygen, and the carboxylic-acid proton is in the preferred syn configuration. The syn configuration of the acidic proton is sacrificed in the higher energy conformation to form an intramolecular hydrogen bond to the amino nitrogen. Evidence of a third conformation of glycine, in which the hydrogens of the amine form an intramolecular hydrogen bond with the oxygen of the acid group, has recently been reported in a matrix IR study.[9,10]

Glycine and alanine are the amino acids with the smallest side chains, a proton and a methyl group, respectively, so their backbone conformations are dominated by intramolecular hydrogen bonding interactions. The isopropyl side chain of valine, however, has greater steric requirements which may influence the backbone conformation. From infrared absorption studies, Iitaka proposed that L-valine has an unusual crystal structure, one in which the unit cell is composed of molecules with two distinct conformations.[12] The difference between the conformations lay solely in the orientation of the isopropyl side chain, which was described by χ_1, the dihedral angle between the protons of the alpha and beta carbon atoms ($H^{\beta}-C^{\beta}-C^{\alpha}-H^{\alpha}$). Iitaka's deduction was proven correct when the crystal structure was determined by X-ray analysis, and the unit cell was found to be composed of molecules with $\chi_1 = 180°$ (trans) and $\chi_1 = 60°$.[13]

Recent ab initio calculations on gas-phase valine[14−16] (geometry optimizations at HF/6-31G*, energy calculations of the resulting structures at MP2/6-31+G*)[15] found 26 unique conformations, four of which lie within 4 kJ mol^{-1} of the global minimum.[15] The most stable conformations possess one of the three intramolecular hydrogen bonding networks found for glycine and alanine: bifurcated amine-to-carbonyl oxygen, bifurcated amine-to-carboxylic acid oxygen, or carboxylic acid proton-to-nitrogen. Three preferred orientations of the isopropyl, with $\chi_1 = 60°$, 180°, or 300°, were found for each backbone conformation. The lowest energy conformation has the bifurcated amine-to-carbonyl oxygen intramolecular hydrogen bond network and has the isopropyl group oriented with $\chi_1 = 292°$. Interestingly, it was found that the energy ordering of the side

† Current address: Optical Technology Division, National Institute of Standards and Technology, Gaithersburg, MD 20899-8441.

10.1021/jp020663y CCC: $22.00
Published on Web 08/07/2002

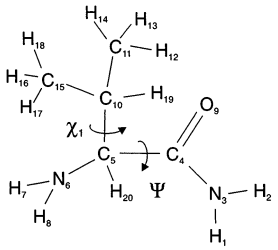

Figure 1. Molecular structure and atomic labels of valinamide.

chain conformations (χ_1) depends on the backbone conformation. The relative energies of the different side chain orientations were found to be in the order 292° < 174° < 64° for the bifurcated amine-to-carbonyl-oxygen backbone conformation, 294° < 72° < 194° for the carboxylic-acid-to-amine conformation, and 173° < 290° < 64° for the bifurcated amine-to-hydroxyl-oxygen conformation.[15] The differences in energy ordering were attributed to the steric requirements of the isopropyl side chain and the interaction between the backbone and the side chain. Three low-energy valine conformations with different intramolecular hydrogen bonding networks have been identified by matrix-isolation infrared spectroscopy.[16]

The current study involves the determination of the structure of the amide derivative of valine, shown in Figure 1. Because polypeptides are joined together by amide linkages, the intramolecular hydrogen bonding networks in peptides are better represented by amino amides than amino acids, and the amino amide derivatives may be viewed as simple peptide models. We have previously determined the conformational structures for alaninamide[17] and prolinamide.[18] Unlike the amino acids, only one gas phase conformation has been observed for each of these molecules. The backbone structure is stabilized by an intramolecular hydrogen bond from an amide proton to the amino nitrogen, and this conformation is unchanged in the alaninamide-water van der Waals complex.[19]

This study of the structure of valinamide represents an extension of our previous amino amide studies. Although both alaninamide and valinamide have hydrophobic side chains, the isopropyl group of valinamide is much larger than the methyl group of alaninamide. We have undertaken this study to address the question of how the steric demands of the side chain may affect the conformation of the backbone.

Experimental Section

Rotational spectra were recorded using a Balle-Flygare type[20] Fourier transform microwave spectrometer described in detail elsewhere.[21] A Fabry−Perot resonant cavity is established by two 36 cm diameter aluminum mirrors with spherical radius of curvature of 84 cm. One of the mirrors is fixed, and the second can be moved with a motorized micrometer to tune to the desired frequency. The maximum separation of the mirrors is 80 cm.

Microwave radiation generated by a Hewlett-Packard 83711B synthesized frequency generator is coupled into the cavity through an L-shaped antenna mounted in the center of one of the mirrors. Molecular emission is detected using the same antenna and frequency reduced by a heterodyne circuit; the frequency range of the spectrometer is 5−18 GHz. The signal is digitized by a Keithley-MetraByte DAS-4101 data acquisition board in a personal computer. National Instruments PC-TIO-10 and PC-LPM-16 counter timer boards generate pulses that control the pin diode switches, valve driver, and motorized micrometer. A windows-based graphical user interface written in Borland C++ is used to control the spectrometer and to analyze the spectra. Sample injection into the cavity is accomplished by a heated nozzle oriented perpendicular to the cavity axis. This orientation of the expansion produces line widths of approximately 30 kHz (full width at half-maximum), with line centers accurate to ±4 kHz.

TABLE 1: Center Frequencies of the Rotational Transitions of Valinamide from Fitting Nuclear Quadrupole Hyperfine Transitions

transition	obsd/MHz	obsd − calcd/kHz
$3_{13}-2_{12}$	7832.882	0.0
$3_{03}-2_{02}$	8090.387	1.5
$3_{21}-2_{20}$	8263.131	−8.8
$3_{13}-2_{02}$	9180.490	3.2
$4_{04}-3_{13}$	9604.724	4.9
$2_{21}-1_{10}$	10310.261	5.4
$2_{20}-1_{10}$	10332.198	−3.8
$4_{13}-3_{12}$	11295.124	−1.3
$4_{14}-3_{03}$	11511.317	−0.3
$5_{05}-4_{14}$	12425.722	2.2
$5_{14}-4_{04}$	13810.320	−3.2

L-Valinamide, liberated from the hydrochloride salt with 1 M NaOH, was incorporated into a supersonic expansion by heating to 120 °C. The backing pressure of the argon carrier gas was typically 1.5 atm. Isotopically labeled species of valinamide were synthesized by a four-reaction step procedure[17,18] using $^{15}NH_4Cl$ and valine-^{15}N or valine-d_8 (Cambridge Isotope Labs). Briefly, these reactions protect the amine group, activate the carbonyl, form the amide, and deprotect the amine. The products of intermediate steps were characterized by melting points and both FTIR and NMR spectroscopy.

Results

Twenty three rotational transitions were observed for the most abundant isotopomer of valinamide, and these transitions were split into many (ca. 10) components spanning up to 3 MHz by nuclear quadrupole coupling from the two ^{14}N nuclei. The nuclear quadrupole hyperfine structure was assigned for eleven rotational transitions (4 *a*-types, 6 *b*-types, and 1 *c*-type). The unsplit center frequencies of the rotational transitions, given in Table 1, were obtained by fitting the hyperfine components to the quadrupole coupling constants for the amino and amide nitrogen nuclei. The frequencies of the hyperfine components are tabulated in the Supporting Information; $(\nu_{obs} - \nu_{calc})_{rms} = 5.9$ kHz for the 99 hyperfine components. The rotational and centrifugal distortion constants derived from fitting the center frequencies of the rotational transitions to the Watson A-reduction Hamiltonian[22] are given in Table 2; $(\nu_{obs} - \nu_{calc})_{rms} = 4.0$ kHz for the fit.

Four isotopically labeled species have also been investigated: valinamide-$^{15}N(3)$, valinamide-$^{15}N(6)$, valinamide-$^{15}N(3)$,$^{15}N(6)$, and valinamide-d_8,$^{15}N(3)$ (deuterium substitution occurring at the six protons of the C^{γ} groups and the hydrogen atoms bound to the α and β carbons). Forty-two rotational transitions were measured for valinamide-$^{15}N(3)$,$^{15}N(6)$. Nuclear quadrupole hyperfine structure was assigned for thirteen rotational transitions of valinamide-$^{15}N(6)$, with $(\nu_{obs} - \nu_{calc})_{rms} = 3.9$ kHz for 46 hyperfine components, and fifteen transitions of valinamide-$^{15}N(3)$, with $(\nu_{obs} - \nu_{calc})_{rms} = 4.4$ kHz for the 63 hyperfine components. The rotational transitions of the deuterated isotope were broadened up to 500 kHz by overlapping nuclear quadrupole hyperfine components arising from the $^{14}N(6)$ and the deuterium nuclei. Because the hyperfine structure could not be resolved, line centers of the rotational transitions were estimated to be at the center of the broadened band. The transition frequencies for the isotopic species are available in the Supporting Information. The rotational transitions of each

TABLE 2: Spectroscopic Constants of Valinamide Isotopic Species

	valinamide	valinamide-^{15}N(6)	valinamide-^{15}N(3)	valinamide-^{15}N(3),^{15}N(6)	valinamide-d_8,^{15}N(3)
A/MHz	3019.242(1)	2963.661(2)	3012.18(2)	2957.1045(2)	2648.144(8)
B/MHz	1473.0587(7)	1472.9358(8)	1451.024(6)	1450.9112(2)	1279.181(6)
C/MHz	1252.5350(8)	1242.921(1)	1236.070(8)	1226.7409(2)	1125.974(3)
Δ_J/kHz	0.17(2)	0.15(2)	0.14(2)	0.164(3)	
Δ_{JK}/kHz		0.3(2)	0.4(2)	0.418(10)	
χ_{aa} [N(6)]/MHz	−3.276(2)		−3.318(2)		
χ_{bb} [N(6)]/MHz	1.400(3)		1.442(2)		
χ_{aa} [N(3)]/MHz	1.640(2)	1.638(2)			
χ_{bb} [N(3)]/MHz	1.141(3)	1.161(3)			
N^a	11	13	15	42	19
$\Delta\nu_{rms}$/kHz	4.0	4.6	3.9	2.4	92.5

[a] Number of center frequencies included in the fit.

TABLE 3: Ab Initio Conformers (MP2/6-31G) of Valinamide**

conformer	χ_1/deg	rel energy/kJ mol^{-1}	ΔI_{rms}/amu Å^2
AAI	71	0.0	51.2
AAII	300	1.2	15.0
AAIII	183	3.4	20.4
BAI	293	4.3	18.2
BAII	177	6.0	17.3
BAIII	59	7.6	55.0

isotopomer were fit to the Watson A-reduction Hamiltonian, and spectroscopic constants for the isotopically labeled species are given in Table 2. The uncertainties reported in Table 2 represent one standard deviation uncertainty arising from fitting the rotational constants to the experimental frequency data.

Structure and Discussion

We performed ab initio calculations using Gaussian 94[23] to identify the likely conformations of valinamide. Geometry optimizations were performed at the UMP2 level of theory with a 6-31G** basis set.[24−26] The calculations identified six conformational minima, four of which lie within 5 kJ mol^{-1} of the global minimum. Backbone conformations with amide-to-amine intramolecular hydrogen bonds (conformers AAI, AAII, and AAIII) were found to be more stable than structures with bifurcated amine-to-carbonyl hydrogen bonds (conformers BAI, BAII, and BAIII). Table 3 lists the relative energies, not corrected for zero-point energies, for the six stable conformations, and representative structures of the two backbone conformations (AA and BA) are shown in Figure 2. Three orientations of the isopropyl group (with χ_1 approximately 60°, 180°, and 300°) were found for each backbone conformation, as was also found for valine. Newman projections of the three isopropyl orientations are shown in Figure 3 for the amide-to-amine hydrogen bonding scheme. Like the valine conformers, the energy ordering of the isopropyl orientations was found to depend on the backbone conformation of valinamide. For the amide-to-amine backbone conformer, the relative energies of the isopropyl orientations is in the order 71° ≈ 300° < 183°, whereas for the amine-to-carbonyl scheme the ordering is 293° < 177° < 59°.

Root-mean square averages of the differences between the experimental moments of inertia and those calculated from the ab initio structures, ΔI_{rms}, where $\Delta I = I_x(\text{exp}) - I_x(\text{calcd})$ and $x = a$, b, and c for each isotopomer, are also given in Table 3. None of the ab initio structures reproduces the experimental moments of inertia, but conformers AAI (the lowest energy structure) and BAIII have ΔI_{rms} values greater than 50 amu Å^2 and are not likely to give rise to the recorded spectra. Because the remaining conformers all have $\Delta I_{rms} \approx 15$ amu Å^2, it is not possible to assign the rotational spectrum to any of the theoretical structures. Moreover, the consistently large values of ΔI_{rms} suggest that none of the theoretical structures adequately describes the structure of the measured conformer.

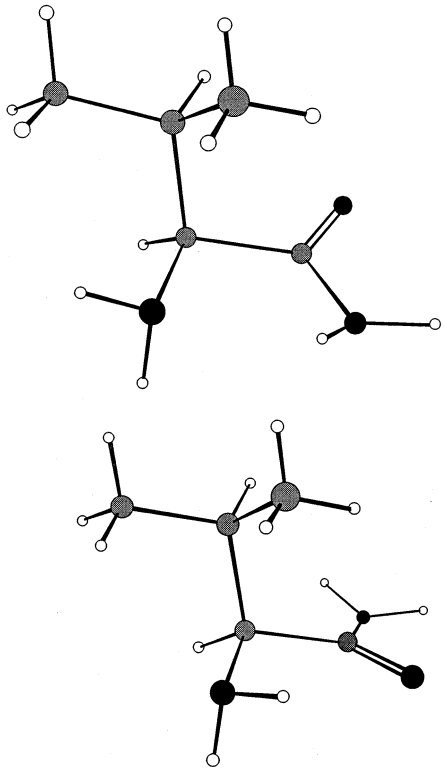

Figure 2. Two intramolecular hydrogen bonding schemes of valinamide: (a) amide-to-amine (AAII); (b) bifurcated amine-to-carbonyl (BAI).

The ab initio conformers AAI, AAII, AAIII, BAI, and BAII were used as starting structures for least-squares fits of the structure to the experimental moments of inertia. In each case, two internal coordinates describing the backbone structure (the angle C(4)−C(5)−N(6) and Ψ, the dihedral angle N(3)−C(4)−C(5)−N(6)) and five internal coordinates describing the orientation of the isopropyl side chain (the angles C(4)−C(5)−C(10), C(5)−C(10)−C(11), and C(5)−C(10)−C(15) and the dihedral angles N(3)−C(4)−C(5)−C(10) and C(4)−C(5)−C(10)−C(11)) were fit using the program STRFITQ.[27] The torsional angle N(3)−C(4)−C(5)−H(20) was adjusted concurrently with N(3)−C(4)−C(5)−C(10), and the torsional angles C(4)−C(5)−C(10)−C(15) and C(4)−C(5)−C(10)−H(19) were adjusted concurrently with C(4)−C(5)−C(10)−C(11). The remaining internal coordinates were fixed at the ab initio values because they were not determined by the limited set of experimental moments of inertia. Structure fits of AAIII, BAI, and BAII were unable to reproduce the experimental moments of inertia and did not

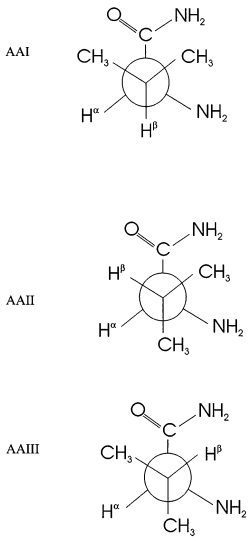

Figure 3. Newman projections of the isopropyl group orientation in the ab initio conformations in the amide-to-amine intramolecular hydrogen bonding scheme.

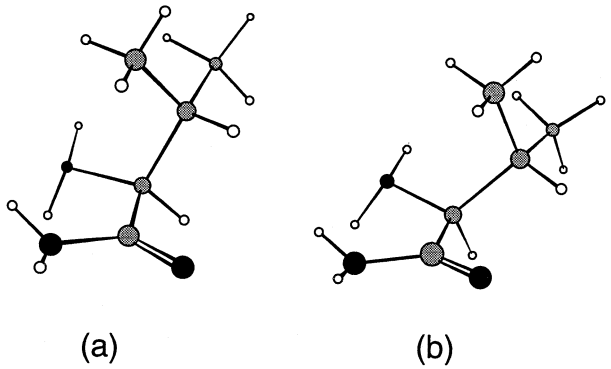

Figure 4. Same-perspective comparison of (a) the ab initio structure of valinamide with $\chi_1 = 300°$ and $\Psi = -9.3°$ and (b) the best-fit structure of valinamide with $\chi_1 = 298°$ and $\Psi = 9.7°$.

converge. The structure fit of conformer AAI converged to a structure that reproduced the experimental data with $\Delta I_{rms} = 0.156$ amu Å^2, but this structure is not plausible because the angles C(4)−C(5)−C(10) and C(5)−C(10)−C(11) increased to 130° and 125°, respectively (the ab initio values for these angles are 110.4° and 111.9°). The best-fit structure of valinamide is derived from fitting conformer AAII; the fit structure reproduces the experimental data with $\Delta I_{rms} = 0.028$ amu Å^2. Whereas the C(4)−C(5)−N(6), C(4)−C(5)−C(10), and C(5)−C(10)−C(11) bond angles remain within 4.1° of the ab initio values, Ψ (the N(3)−C(4)−C(5)−N(6) dihedral angle) changes from −9.3° to +9.7(30)° and the N(3)−C(4)−C(5)−C(10) dihedral angle changes from 113.3° to 140.2(30)°. The relative orientation of the side chain with respect to the backbone is relatively unchanged by the fitting because the C(4)−C(5)−C(10)−C(11) dihedral angle is −65.7(30)° after fitting (−64.7° in the ab initio structure); χ_1 is 300.1° in the ab initio structure and 298.2(30)° in the fit structure. This orientation places one of the C$^\gamma$ methyl groups above the backbone plane, whereas the second C$^\gamma$ methyl group is directed away from the backbone structure; see Figure 4. Structural parameters of the ab initio and least-squares fit structures are given in Tables 4−6.

The parallel increase of Ψ and the dihedral angle N(3)−C(4)−C(5)−C(10) upon fitting may be described as arising from a counterclockwise rotation of amide group about the C(4)−C(5) bond (with respect to the C(5)−N(6) and C(5)−C(10) bonds). As Ψ increases from −9.3° to +9.7(30)°, C(11) (above the backbone) moves farther from the amide, as shown in Figure 4 and illustrated by an increase in the C(11)−N(3) distance from 3.474 Å in the ab initio structure to 3.864(46) Å in the fit structure. The larger C(11)−N(3) distance suggests that long-range repulsive interactions between the amide and one of the

TABLE 4: Bond Lengths (Å) of the ab Initio and Best-Fit Structures of Valinamide

	ab initio (AAII)	best fit
H(1)−N(3)	1.010	1.010
H(2)−N(3)	1.009	1.009
N(3)−C(4)	1.366	1.366
C(4)−O(9)	1.223	1.223
C(4)−C(5)	1.533	1.533
C(5)−C(10)	1.543	1.543
C(5)−H(20)	1.104	1.104
C(5)−N(6)	1.468	1.468
N(6)−H(7)	1.016	1.016
N(6)−H(8)	1.017	1.017
C(10)−C(11)	1.531	1.531
C(11)−H(12)	1.095	1.095
C(11)−H(13)	1.095	1.095
C(11)−H(14)	1.096	1.096
C(10)−C(15)	1.531	1.531
C(15)−H(16)	1.098	1.098
C(15)−H(17)	1.096	1.096
C(15)−H(18)	1.096	1.096
C(10)−H(19)	1.099	1.099

TABLE 5: Bond Angles (deg) of the ab Initio and Best-Fit Structures of Valinamide

	ab initio (AAII)	best fit
H(1)−N(3)−H(2)	119.8	119.8
H(2)−N(3)−C(4)	116.8	116.8
N(3)−C(4)−O(9)	124.4	124.4
N(3)−C(4)−C(5)	114.5	114.5
C(4)−C(5)−H(20)	105.2	105.2
C(4)−C(5)−N(6)	111.3	114.0(30)
C(4)−C(5)−C(10)	108.2	111.5(30)
C(5)−N(6)−H(7)	109.0	109.0
C(5)−N(6)−H(8)	108.7	108.7
C(5)−C(10)−C(11)	112.2	108.8(30)
C(5)−C(10)−C(15)	111.7	112.1(30)
C(5)−C(10)−H(19)	104.8	104.8
C(10)−C(11)−H(12)	111.5	111.5
C(10)−C(11)−H(13)	110.9	110.9
C(10)−C(11)−H(14)	110.3	110.3
C(10)−C(15)−H(16)	111.8	111.8
C(10)−C(15)−H(17)	111.4	111.4
C(10)−C(15)−H(18)	110.4	110.4

TABLE 6: Bond Torsion Angles (deg) of the ab Initio and Best-Fit Structures of Valinamide

	ab initio (AAII)	best fit
H(1)−N(3)−C(4)−C(5)	−16.1	−16.1
H(2)−N(3)−C(4)−C(5)	−168.1	−168.1
H(1)−N(3)−C(4)−O(9)	164.4	164.4
Ψ = N(3)−C(4)−C(5)−N(6)	−9.3	+9.7(30)
N(3)−C(4)−C(5)−C(10)	113.3	140.2(30)
N(3)−C(4)−C(5)−H(20)	−132.6	−105.7
C(4)−C(5)−N(6)−H(7)	171.5	171.5
C(4)−C(5)−N(6)−H(8)	−74.2	−74.2
C(4)−C(5)−C(10)−C(11)	−64.7	−65.7(30)
C(4)−C(5)−C(10)−C(15)	169.9	168.9(30)
C(4)−C(5)−C(10)−H(19)	53.0	52.0(30)
C(5)−C(10)−C(11)−H(12)	58.3	58.3
C(5)−C(10)−C(11)−H(13)	−62.2	−62.2
C(5)−C(10)−C(11)−H(14)	178.1	178.1
C(5)−C(10)−C(15)−H(16)	69.2	69.2
C(5)−C(10)−C(15)−H(17)	−52.1	−52.1
C(5)−C(10)−C(15)−H(18)	−172.2	−172.2
χ_1 = H(19)−C(10)−C(5)−H(20)	300.1	298.2(30)

TABLE 7: Principal-Axis-System Coordinates (Å) of the Nitrogen Atoms from Kraitchman Analysis, ab Initio Calculations (AAII), and the Best-Fit Structure

	ab initio	best fit	Kraitchman
		N(3)	
a	−2.022	−2.259	±2.271(1)
b	0.600	0.575	±0.508(3)
c	0.626	0.350	±0.289(5)
		N(6)	
a	0.212	0.169	±0.134(11)
b	1.730	1.760	±1.767(1)
c	−0.223	0.163	±0.130i

side-chain methyl groups may be responsible for the increase in Ψ. The increase in Ψ also increases the N−N separation to 2.708(27) Å, from 2.643 Å in the ab initio structure, and the N−N distance in the fit structure of valinamide is longer than the comparable heavy-atom separation in the experimental structure of alaninamide (2.678 Å),[17] although the uncertainty in the fit value for valinamide makes the significance of this increase questionable.

The changes in the dihedral angles N(3)−C(4)−C(5)−N(6) (Ψ) and N(3)−C(4)−C(5)−C(10) are experimentally distinguishable because the ab initio and best-fit values differ by much more than the uncertainty, which we estimate to be 3° (we also estimate the uncertainty to be ±3° for the fitted angles because of the large number of constrained parameters). Also, the fit structure reproduces the experimental moments of inertia within experimental uncertainty whereas the theoretical structure AAII predicts spectra that are substantially different from the measured spectra. Additional evidence supporting the fit structure comes from analyzing the coordinates of the two nitrogen atoms. Because spectra of two singly labeled nitrogen isotopomers were measured, Kraitchman's equations for single isotopic substitution[28,29] were used to independently calculate the absolute values of the atomic coordinates for the nitrogen atoms in the principal axis system of the parent isotopic species. The Kraitchman coordinates are given in Table 7 and compared to the nitrogen atomic coordinates of the ab initio and least-squares-fit models. The imaginary value for the Kraitchman *c*-coordinate of the amino nitrogen is not unusual and arises from zero-point vibrational averaging of a small coordinate value. Although there are large differences between the ab initio and Kraitchman nitrogen coordinates, the least-squares-fit coordinates fall within 0.07 Å of the Kraitchman coordinates. The modest differences between the least-squares-fit and Kraitchman coordinates are primarily attributed to the fit structure and arise because of the large number of structural parameters that are constrained to ab initio values in the fit. Some of the differences between the least-squares-fit and Kraitchman coordinates may also arise from different treatments of zero-point vibrational averaging in the two methods of analysis.

It is evident from Table 7 that the *c*-coordinate of N(6) changes sign during the fitting process, from −0.223 to +0.163 Å, presumably as a result of fitting Ψ. The *a*-coordinate of N(3) also changes from −2.022 to −2.259 Å, so the least-squares fitting was not limited to adjustments of small and uncertain atomic coordinate values. Large changes were also observed for the values of the *b*- and *c*-coordinates of the γ carbons and hydrogens, and we expect these coordinates to be well determined from fitting to the moments of inertia of valinamide-d_8,^{15}N(3). Thus the fit structure is reliable and it reproduces the experimental data better than the theoretical structure.

An MP2/6-31G** single point calculation finds that the best-fit structure is 17 kJ mol^{-1} higher in energy than structure AAI, but this value is likely to be greatly inflated by energy contributions from the small and uncertain changes in the angles C(4)−C(5)−N(6), C(4)−C(5)−C(10), C(5)−C(10)−C(11), C(5)−C(10)−C(15), and the dihedral angles C(4)−C(5)−C(10)−C(11), C(4)−C(5)−C(10)−C(15), and C(4)−C(5)−C(10)−H(19). A geometry optimization (MP2/6-31G**) of the best-fit structure moves away from the fit geometry and converges on the AAII structure. There are several possible reasons why the fit structure differs from the ab initio structure. Despite an optimization beginning from the fit structure, we cannot eliminate the possibility that our optimizations missed a conformational minimum or plateau near the fit structure. Alternatively, it may be that the potential energy surface for the Ψ torsion of the backbone is too steep with this basis set and that the amino amide backbone is more flexible than the ab initio model. A recent high-resolution spectroscopic structure of ethyl sulfide also had significant differences with the ab initio values for the torsional angles that define conformation.[30] The agreement between the fit structure and the Kraitchman coordinates for valinamide makes it unlikely that the differences with the theoretical structure arise predominantly from zero-point averaging along a large-amplitude vibrational coordinate. In any case, if the increase in potential energy along the Ψ coordinate is on the order of 10 kJ mol^{-1}, zero-point vibrational averaging is expected to be minimal. No internal rotor state transitions were observed in long-range spectral scans, so methyl internal rotation tunneling is also quenched by a high barrier.[17,19] The effect of the isopropyl side chain on the backbone structure of valinamide warrants additional theoretical studies to better characterize the potential energy surface and explore basis set effects.

The ab initio calculations predict that there is a second stable structure 1.15 kJ mol^{-1} lower in energy than the observed conformation (Table 3). If the barrier to interconversion to the lower energy conformer is greater than the available thermal energy, then the relative populations of these conformers in the expansion will reflect their populations in the heated sample chamber.[31] The intensities of rotational transitions observed by Fourier transform microwave spectroscopy are directly proportional to both the conformer population and the magnitude of the dipole moment projections onto the principal inertial axes.[32] Dipole moment projections were estimated from the ab initio calculations to be $\mu_a = 0.1$ D, $\mu_b = 3.7$ D, and $\mu_c = 0.1$ D for AAI and $\mu_a = 1.7$ D, $\mu_b = 3.1$ D, and $\mu_c = 1.1$ D for AAII; the calculated dipole moment projections for AAII (the theoretical structure most similar to the fit structure) agree well with the observation of a strong *b*-type spectrum with weaker *a*- and *c*-type transitions. The population and dipole moment analysis, however, suggests that the *b*-type spectrum of AAI should be 70% stronger than the observed *b*-type spectrum of AAII. No additional transitions were recorded that could be assigned to a second valinamide conformation; moreover, no new valinamide transitions could be identified from additional spectral searches in the 13−22 GHz range using the Fourier transform microwave spectrometers at NIST.[33] Our spectroscopic results, then, suggest that the fitted structure may be the lowest energy conformation and that the remaining conformers are more than 3 kJ mol^{-1} higher in energy (assuming that we would have assigned transitions with 40% of the intensity of the observed spectrum).

Conclusions

Rotational spectra have been recorded for five isotopic species of the amino acid derivative valinamide. Internal coordinates describing the structure of the backbone and the orientation of

the isopropyl side chain were fit to moments of inertia derived from fitting the spectra to Watson A-reduction Hamiltonians. The best-fit structure is characterized by an intramolecular hydrogen bond from the amide to the amine and the side chain is oriented with $\chi_1 = 298°$. Atomic coordinates of the nitrogen atoms, as calculated from Kraitchman's equations for single isotopic substitution, support the best-fit structure. This structure differs from the lowest energy theoretical models because of an increase in the value of Ψ, the torsional angle of the backbone.

Note Added in Proof. Ab initio optimizations of the structure of valinamide (RHF/6-311++G**) were performed by Prof. Attila G. Csa'sza'r and Ms. Eszter Czinki while this manuscript was in final review. They found 14 unique conformational minima, and their global energy minimum structure reproduces the experimental spectroscopic constants well ($\Delta I_{rms} = 2.34$ amu Å^2 for valinamide, valinamide-^{15}N(3), valinamide-^{15}N(6), and valinamide-^{15}N(3),^{15}N(6)). A-reduction centrifugal distortion constants, computed at the same level, support the experimental values given in Table 2. For the normal isotopic species these constants are calculated to be $\Delta_J = 0.16$ kHz, $\Delta_{JK} = 0.038$ kHz, $\Delta_K = 0.058$ kHz, $\delta_J = 0.012$ kHz, and $\delta_K = 0.27$ kHz.[34]

Acknowledgment. This work was supported by a grant from the U. S. National Science Foundation (CHE-9700833). The authors also wish to thank Prof. Attila G. Csa'sza'r and Ms. Eszter Czinki for their interest in the structure of valinamide and for the results of their ab initio optimizations.

Supporting Information Available: Five tables of transition frequencies for isotopic species of valinamide. This information is available free of charge via the Internet at http://pubs.acs.org.

References and Notes

(1) (a) Brown, R. D.; Godfrey, P. D.; Storey, J. W. V.; Bassez, M.-P. *J. Chem. Soc., Chem. Commun*. **1978**, 547−548. (b) Suenram, R. D.; Lovas, F. J. *J. Mol. Spectrosc*. **1978**, *72*, 372.
(2) Suenram, R. D.; Lovas, F. J. *J. Am. Chem. Soc.* **1980**, *102*, 7810.
(3) Godfrey, P. D.; Brown, R. D. *J. Am. Chem. Soc.* **1995**, *117*, 2019.
(4) Lovas, F. J.; Kawashima, Y.; Grabow, J.-U.; Suenram, R. D.; Fraser, G. T.; Hirota, E. *Astrophys. J.* **1995**, *455*, L201.
(5) McGlone, S. J.; Elmes, P. S.; Brown, R. D.; Godfrey, P. D. *J. Mol. Struct*. **1999**, *485*/*486*, 225.
(6) Godfrey, P. D.; Firth, S.; Hatherley, L. D.; Brown, R. D.; Pierlot, A. P. *J. Am. Chem. Soc.* **1993**, *115*, 9687.
(7) Iijima, K.; Tanaka, K.; Onuma, S. *J. Mol. Struct*. **1991**, *246*, 257.
(8) Iijima, K.; Beagley, B. *J. Mol. Struct*. **1991**, *248*, 133.
(9) Reva, I. D.; Plokhotnichenko, A. M.; Stepanian, S. G.; Ivanov, A. Y.; Radchenko, E. D.; Sheina, G. G.; Blagoi, Y. P. *Chem. Phys. Lett*. **1995**, *232*, 141.
(10) Stepanian, S. G.; Reva, I. D.; Radchenko, E. D.; Rosado, M. T. S.; Duarte, M. L. T. S.; Fausto, R.; Adamowicz, L. *J. Phys. Chem. A* **1998**, *102*, 1041.
(11) Stepanian, S. G.; Reva, I. D.; Radchenko, E. D.; Adamowicz, L. *J. Phys. Chem. A* **1998**, *102*, 4623.
(12) Tsuboi, M.; Takenishi, T.; Iitaka, Y. *Bull. Chem. Soc. Jpn.* **1959**, *32*, 305.
(13) Torii, K.; Iitaka, Y. *Acta Crystallogr*. **1970**, *B26*, 1317.
(14) Schäfer, L.; Kulp-Newton, S. Q.; Siam, K.; Klimkowski, V. J.; Van Alsenoy, C. *J. Mol. Struct*. (*THEOCHEM*) **1990**, *209*, 373.
(15) Shirazian, S.; Gronert, S. *J. Mol. Struct*. (*THEOCHEM*) **1997**, *397*, 107.
(16) Stepanian, S. G.; Reva, I. D.; Radchenko, E. D.; Adamowicz, L. *J. Phys. Chem. A* **1999**, *103*, 4404.
(17) Lavrich, R. J.; Farrar, J. O.; Tubergen, M. J. *J. Phys. Chem. A* **1999**, *103*, 4659.
(18) Kuhls, K. A.; Centrone, C. A.; Tubergen, M. J. *J. Am. Chem. Soc.* **1998**, *120*, 10194.
(19) Lavrich, R. J.; Tubergen, M. J. *J. Am. Chem. Soc*. **2000**, *122*, 2938.
(20) Balle, T. J.; Flygare, W. H. *Rev. Sci. Instrum*. **1981**, *52*, 33.
(21) Tubergen, M. J.; Flad, J. E.; Del Bene, J. E. *J. Chem. Phys*. **1997**, *107*, 2227.
(22) Watson, J. K. G. *J. Chem. Phys*. **1967**, *46*, 1935.
(23) Frisch, M. J.; Trucks, G. W.; Schlegal, H. B.; Gill, P. M. W.; Johnson, B. G.; Robb, M. A.; Montgomery, J. A.; Raghavachari, K.; Al-Laham, M. A.; Zakrzewski, V. G.; Oritz, J. V.; Foresman, J. B.; Cioslowski, J.; Stefanov, B. B.; Nanayakkara, A.; Challacombe, M.; Peng, C. Y.; Ayala, P. Y.; Chen, W.; Wong, M. W.; Andres, J. L.; Replogle, E. S.; Gomperts, R.; Martin, R. L.; Fox, D. J.; Binkley, J. S.; Defrees, D. J.; Baker, J.; Stewart, J. P.; Head-Gorden, M.; Gonzalez, C.; Pople, J. A. *Gaussian94*, revision E.3; Gaussian, Inc.: Pittsburgh, PA, 1995.
(24) Møller, C.; Plesset, M. S. *Phys. Rev*. **1934**, *46*, 618.
(25) Pople, J. A.; Binkley, J. S.; Seeger, R. *Int. J. Quantum Chem. Symp*. **1976**, *10*, 1.
(26) Petersson, G. A.; Bennett, A.; Tensfeldt, T. G.; Al-Laham, M. A.; Shirley, W. A.; Mantzaris, J. *J. Chem. Phys*. **1988**, *89*, 2193.
(27) Schwendeman, R. H. Critical Evaluation of Chemical and Physical Structural Information; Lide, D. R., Paul, M. A., Eds.; National Academy of Sciences: Washington, DC, 1974.
(28) Kraitchman, J. *Am. J. Phys*. **1953**, *21*, 17.
(29) Gordy, W.; Cook, R. L. *Microwave Molecular Spectra*; Wiley: New York, 1984.
(30) Plusquellic, D. F.; Suenram, R. D.; Maté, B.; Jensen, J. O.; Samuels, A. C. *J. Chem. Phys*. **2001**, *115*, 3057.
(31) Ruoff, R. S.; Klots, T. D.; Emilsson, T.; Gutowsky, H. S. *J. Chem. Phys*. **1990**, *93*, 3142.
(32) Fraser, G. T.; Suenram, R. D.; Lugez, C. L. *J. Phys. Chem. A* **2000**, *104*, 1141.
(33) Lavrich, R. J. Unpublished results.
(34) Csa'sza'r, A. G.; Czinki, E., private communication.